1

Introduction

This chapter presents a brief introduction to metal powder–based additive manufacturing (AM). The history and fundamentals of AM are first highlighted. Seven categories of AM techniques with their representative processes and commercial companies are then presented, followed by an overview of the types of metal powder–based AM techniques. Next, the types of post-processing treatments for metal AM parts are illustrated. Powder properties and characterization methods are also discussed comprehensively. Finally, the challenges and future trends of metal powder–based AM are outlined.

1.1 History and Fundamentals of AM

Additive manufacturing (AM), commonly known as three-dimensional (3D) printing, has emerged as a revolutionary technology capable of fabricating parts with complex geometries in a layer-by-layer manner, thereby granting extensive freedom of design (Martin et al. 2017; Kelly et al. 2019; Zhang et al. 2019). The term "additive manufacturing" describes "the process of joining materials to make parts from 3D model data, usually layer upon layer, as opposed to subtractive manufacturing and formative manufacturing methodologies", according to the ISO/ASTM 52900 standard (ISO and ASTM International 2015). ISO and ASTM are the abbreviations for the International Standards Organization and the American Society for Testing and Materials, respectively. The most commonly used term before AM was "rapid prototyping", which is currently considered outdated because of the increasingly extensive applications of the process.

The advent of AM marks an important milestone in the history of manufacturing. In 1987, Stereolithography Apparatus-1, the first commercial AM system, was launched by 3D Systems in the United States. The system enabled the printing of 3D parts from a computer-aided design (CAD) model for the first time. Other AM techniques were introduced for commercial purposes soon thereafter, which include fused deposition modeling, selective deposition lamination, selective laser sintering, and laminated object manufacturing. Machines operating based on the inkjet printing process began appearing on the market in 1996. In 1998, Optomec delivered the first laser engineered net shaping metal powder system capable of producing

Metal Powder–Based Additive Manufacturing, First Edition. Kun Zhou and Changjun Han.

near-fully dense metal parts. Meanwhile, in 1999, a selective laser melting system was initiated by Fockele & Schwarze of Germany.

The expiry of old AM patents, such as the fused deposition modeling technique (which expired in 2009), has led to a surge in the number of low-cost personal AM machines on the consumer market, some of which can even be assembled by hand. Moreover, the rise of online platforms, such as open-source communities where AM design files are shared freely, further improves the accessibility of 3D printing technology. In 2014, the number of AM patents that expired has reached a peak, which has led to a greater variety of low-cost machines flooding the consumer market.

Over the years, AM has evolved from a tool primarily used for visualization (i.e. rapid prototyping) into a well-recognized technology for producing functional parts with desirable properties. Before printing, a 3D model is constructed via CAD and mathematically sliced into ultrathin printed layers along the build direction. Subsequently, the layers are printed according to their predefined shapes, with consecutive layers bonding to each other.

AM also provides a cost-effective option for low-volume customized production, which differs from conventional mold jetting methods. Parts comprising multiple components can be redesigned as single units and fabricated efficiently without assembly (Chua and Leong 2017). The distinct ability of this process to manufacture complex shapes and structures has already rendered it invaluable for producing prototypes or parts in industries including aerospace, military, biomedical, automotive, electronics, energy, molding, building and construction, marine and offshore, education, art, robotics, environment, and social culture.

AM is also perceived as an environmentally sustainable manufacturing technology, as it can potentially reduce up to 525.5 Mt of total carbon dioxide emissions by 2025 compared to conventional processes (Gebler et al. 2014; Ribeiro et al. 2020). Furthermore, in terms of product development, AM can reduce up to 70% of development costs and time-to-market by up to 90% compared to conventional processes (Gibson et al. 2014). With such remarkable benefits, the global market for AM is projected to reach nearly US$23 billion by 2023, with a compound annual growth rate of 22% (Tan et al. 2020).

1.2 AM Techniques

AM technologies have been classified into seven broad categories according to the ISO/ASTM 52900 standard, namely, vat photopolymerization, material jetting, material extrusion, powder bed fusion (PBF), directed energy deposition (DED), binder jetting, and sheet lamination techniques (ISO and ASTM International 2015), as shown in Figure 1.1. Table 1.1 provides an overview of the representative processes and commercial companies of these AM categories.

The vat photopolymerization technique utilizes radiation (e.g. ultraviolet [UV] and visible light) to selectively polymerize liquid photosensitive resins in a vat to form high-resolution solid 3D structures. It includes various processes such as stereolithography (Hull 1986), digital light processing (Kuang et al. 2019), continuous liquid interfase production (Tumbleston et al. 2015), two-photon photopolymerization

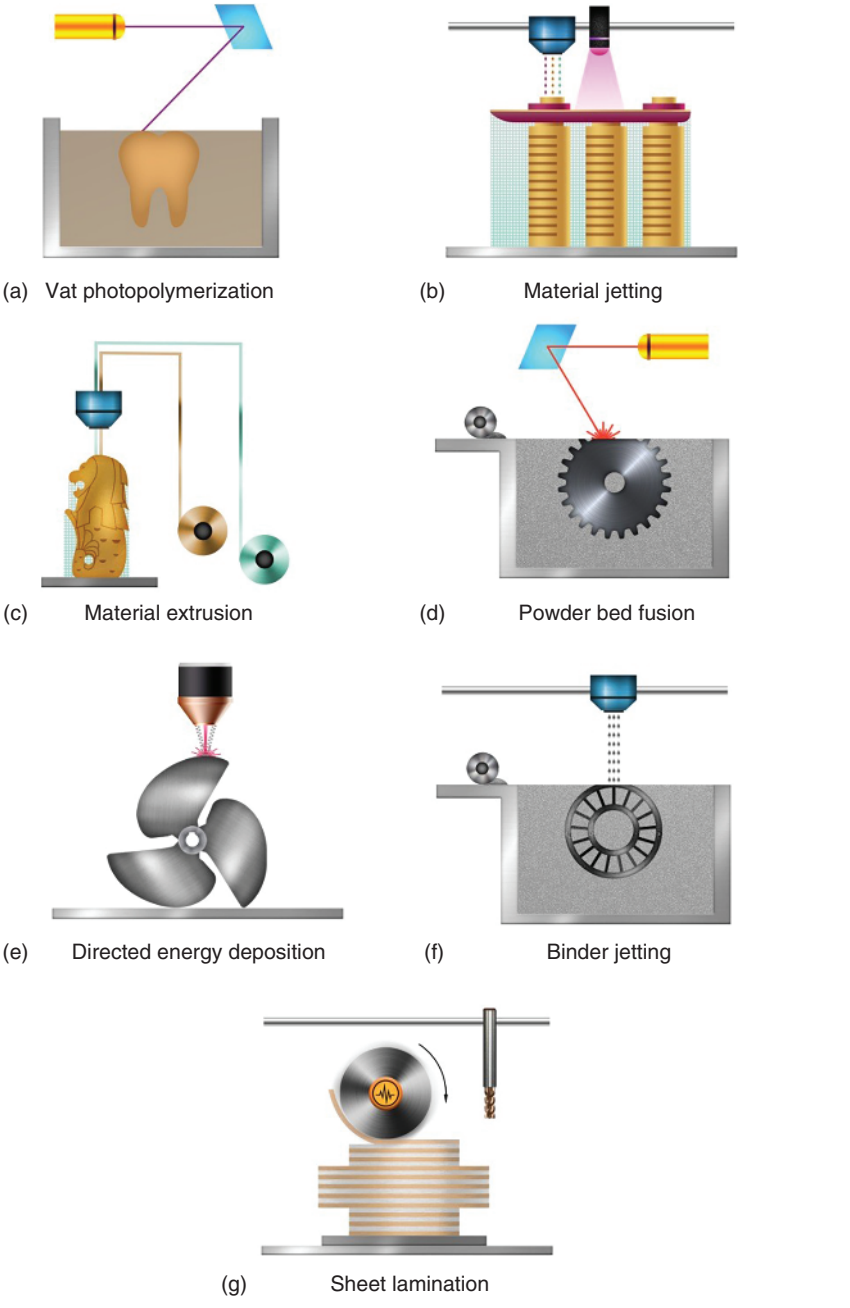

Figure 1.1 Schematics of the seven broad categories of AM technologies according to the ISO/ASTM 52900 standard. Source: ISO and ASTM International (2015)/ISO.

Table 1.1 AM categories, and their representative processes and commercial companies.

AM categories	Representative AM processes	Representative commercial companies	
Vat photopolymerization	Stereolithography	USA	3D Systems, Stratasys, Carbon, Formlabs
	Digital light processing		
	Continuous liquid interface production	Germany	Envisiontec
	Computed axial lithography	China	UnionTech, ZRapid
	Two-photon photopolymerization	France	Prodways
	High-area rapid printing	Australia	Lithoz
		Netherlands	Admatec
		Italy	Sisma, DWS
		Denmark	AddiFab
Material jetting	PolyJet	USA	3D Systems, Stratasys, Optomec, Solidscape, nScrypt
	MultiJet		
	Aerosol jet		
	NanoParticle jetting	Israel	Xjet, Nano Dimension
	Electrohydrodynamic jetting	Japan	Mimaki
Material extrusion	Fused deposition modeling	USA	Stratasys, Markforged, Essentium, Robocasting, Cincinnati
	(Fused filament fabrication)		
	Direct ink writing		
	3D dispensing	Germany	Arburg, BigRep
	(3D plotting)	Netherlands	Ultimaker
Powder bed fusion	Laser powder bed fusion	USA	3D Systems, HP Inc., GE Additive, Velo3D
	(Selective laser melting)		
	(Direct metal laser sintering)	Germany	SLM Solutions, EOS, Trumpf, Voxeljet
	Electron beam melting		
	Selective laser sintering	China	Bright Laser Technologies, Farsoon Technologies, Eplus 3D, Laseradd
	Multi jet fusion		
	High speed sintering	UK	Renishaw
		Italy	Sisma
Directed energy deposition	Laser-based directed energy deposition (Laser engineered net shaping)	USA	Optomec, Sciaky, Addere, Formalloy
	(Laser metal deposition)	Germany	Trumpf, DMG Mori
	Laser wire additive manufacturing	China	Bright Laser Technologies
	Wire arc additive manufacturing	France	BeAM
		Australia	AML3D
	Electron beam freeform fabrication (Electron beam additive manufacturing)	Netherlands	MX3D
		Japan	Sodick
		South Korea	InssTek
		Spain	Addilan

Table 1.1 (Continued)

AM categories	Representative AM processes	Representative commercial companies	
Binder jetting	Binder jetting	USA	3D Systems, HP Inc., Exone, Desktop Metal, Digital Metal
		Germany	Voxeljet
		China	Long Yuan
		UK	Raplas
Sheet lamination	Laminated object manufacturing Ultrasonic additive manufacturing Selective deposition lamination Composite-based additive manufacturing	USA	Fabrisonic, Evolve Additive, Impossible Objects

(Saha et al. 2019), high-area rapid printing (Walker et al. 2019), and computed axial lithography (Kelly et al. 2019). Representative companies for vat photopolymerization include 3D Systems (USA), Carbon (USA), Envisiontec (Germany), Lithoz (Australia), and UnionTech (China).

Figure 1.1a illustrates the top-down stereolithography process, a typical vat photopolymerization technique. Stereolithography is a common vat photopolymerization technique that utilizes an UV laser source positioned above or underneath a resin vat to selectively cure the exposed layer.

The material jetting technique is analogous to traditional two-dimensional (2D) inkjet printing, in which liquid materials (e.g. photosensitive resins, thermoplastics, wax, and reactive materials) are deposited from inkjet printheads onto a build platform through either a drop-on-demand or a continuous approach and subsequently solidified through photopolymerization, cooling, etc. This technique is employed in commercialized systems such as PolyJet, MultiJet, Aerosol Jet, and NanoParticle Jet, as well as non-commercialized systems based on electrohydrodynamic jetting.

Figure 1.1b shows a schematic of the material jetting technique. For example, in the PolyJet system, multiple depositions of photosensitive build materials and support materials (to form the support structures within the printed parts) in the form of droplets are made by nozzles in the printhead before undergoing UV curing. During post-processing, the support structures are removed through mechanical (cutting with a water jet system) and/or chemical (dissolving with a solvent) procedures. Representative companies of material jetting include Stratasys (USA), 3D Systems (USA), Optomec (USA), Xjet (Israel), and Nano Dimension (Israel).

The material extrusion technique typically involves a continuous extrusion of polymer filaments, viscous inks, or even polymer pellets through a heated nozzle onto a build platform, on which the extruded molten material subsequently

solidifies. Fused deposition modeling (also known as fused filament fabrication) and direct ink writing are the key representative processes in this category. The former utilizes thermoplastic filaments and pellets as feedstock materials, while the latter employs viscous inks such as pastes and concentrated polymer solutions (Truby and Lewis 2016). Recent studies have also established the significant potential of fused deposition modeling in printing metal parts. For example, in one such study, printable filaments were prepared through the extrusion of a polyolefin-based binder mixed with 59 vol.% Ti–6Al–4 V powder and then fabricated into parts using the Renkforce 1000 printer (Zhang et al. 2020). In addition, solvent debinding, thermal debinding, and sintering were also conducted to densify the printed parts. Representative companies of material extrusion include Stratasys (USA), Markforged (USA), Essentium (USA), Robocasting (USA), and Ultimaker (Netherlands).

Figure 1.1c illustrates the fused deposition modeling process, a representative material extrusion technique. The build material and the support material, in the form of thermoplastic filaments, are heated to the molten state in the nozzles, extruded, and solidified on the build platform. The support structures are removed through mechanical and/or chemical procedures during post-processing.

The PBF technique utilizes a heat source (e.g. electron beam or laser beam) to coalesce metal, polymer, or ceramic powder particles in a powder bed to build 3D objects, and it can theoretically process any powder–based materials on the condition that the corresponding powder particles can be fused or melted through heating. The technique can be categorized into laser powder bed fusion (LPBF) (also widely known as selective laser melting), electron beam melting (EBM), selective laser sintering, multi jet fusion, and high speed sintering processes. LPBF and EBM are mainly employed to print pure metals, alloys, and metal matrix composites (Han et al. 2020a, 2020b), while the selective laser sintering, multi jet fusion, and high speed sintering processes are typically implemented to treat polymers and their composites. Representative commercial companies of PBF include SLM Solutions (Germany), EOS (Germany), Trumpf (Germany), 3D Systems (USA), GE Additive (USA), Renishaw (UK), Bright Laser Technologies (China), and Farsoon Technologies (China).

Figure 1.1d presents a typical PBF process, LPBF, which utilizes a laser beam to selectively melt metal powder particles in the powder bed. The molten metal particles coalesce and solidify to form the printed part. While unmelted powder particles can serve as support, support structures are generally required to be printed to ensure the good printability of overhanging structures of a part.

The DED technique utilizes a laser beam, an electron beam, or an electric arc to melt metal powders or wires upon their deposition along the printing paths (Bermingham et al. 2015; Li et al. 2021). The technique includes processes such as laser-based directed energy deposition (L-DED) (also widely known as laser engineered net shaping and laser metal deposition), laser wire additive manufacturing (LWAM), wire arc additive manufacturing (WAAM), and electron beam freeform fabrication (EBF^3, also known as electron beam AM). The L-DED process is commonly employed to print parts using powders, while the other four processes

employ wires for printing. Examples of representative companies for DED include Optomec (USA), Sciaky (USA), DMG Mori (Germany), Trumpf (Germany), BeAM (France), and Bright Laser Technologies (China).

Figure 1.1e illustrates a typical DED process, L-DED, in which metal powder particles are delivered through channels in a nozzle and melted by a laser beam upon deposition onto a freeform substrate. The molten metal particles subsequently solidify to form the printed part.

The binder jetting technique utilizes one or more inkjet printheads to deposit droplets of a liquid polymer binder onto ceramic or metal powder particles in a powder bed and selectively glue them together to build 3D objects (Mostafaei et al. 2017). The droplets can be deposited through a single-pass or multi-pass printing strategy. Post-processing procedures, such as curing, de-powdering, infiltration, and sintering, are often required for green parts printed through this technique. Examples of commercialized companies specializing in binder jetting include Exone (USA), Hewlett–Packard (USA), Desktop Metal (USA), Digital Metal (USA), 3D Systems (USA), Voxeljet (Germany), and Long Yuan (China).

Figure 1.1f demonstrates a metal binder jetting (MBJ) process, in which a layer of metal powder particles is spread by a roller across the build platform, and a liquid binder is then selectively deposited to bond specific regions of the powder layer.

The sheet lamination technique can be employed to fabricate 3D objects by stacking and laminating thin sheets of materials (e.g. paper, metal sheets, ceramic tapes, woven fiber composite sheets, and thermoplastic foils) through different bonding (e.g. adhesive bonding, thermal bonding, and ultrasonic welding) and cutting (e.g. computer numerical control [CNC] milling, laser cutting, and water jet cutting) strategies. According to the ISO/ASTM standard, representative processes of the sheet lamination technique include laminated object manufacturing and ultrasonic AM. Laminated object manufacturing was the first commercialized sheet lamination process and was initially implemented to bond kraft paper. Subsequently, the applicability of this process for bonding plastic/metal tapes and foils has been investigated. Meanwhile, the ultrasonic AM process is commonly utilized for printing parts from metal foils and sheets (Dehoff and Babu 2010). In addition to the two aforementioned processes, a novel sheet lamination process, friction stir AM, is currently in development. In this process, metal plates are utilized as feedstock materials. A stirring pin is inserted into a newly added metal plate at high rotation rates, and the resultant friction between the stirring pin and the plate produces heat that softens and bonds the plate to the previous plate. Representative companies for sheet lamination include Fabrisonic (USA), Evolve Additive (USA), and Impossible Objects (USA).

Figure 1.1g presents a diagram of the sheet lamination process, ultrasonic AM, in which each layer of a metal foil is laid and bonded to the previous layer through ultrasonic welding. This process involves the actuation of a cylindrical sonotrode with an ultrasonic transducer to induce a scrubbing motion of the sonotrode. At the same time, a downward force is applied to the metal foils. The sonotrode rolls along the length of the foils due to the downward force, and ultrasonic vibrations are applied along the width of the foils through the sonotrode. Friction can be produced

between the metal foils through the interaction of the downward force and ultrasonic vibrations. Bonding is achieved through disruption of the oxide layers between the metal foils utilizing friction, thereby promoting nascent metal-to-metal contact. The metal layer is subsequently cut through CNC milling to obtain the desired geometry, and the cycle is repeated until the metal part is completed.

1.3 Metal Powder–Based AM

Powder–based AM is an important subset of the AM family for manufacturing parts using powders as feedstock materials, and it employs the PBF, DED, and binder jetting techniques. In particular, LPBF, EBM, L-DED, and MBJ are commonly adopted powder–based AM processes for printing metal parts. LPBF, EBM, and L-DED share similar features, such as the usage of high-energy heat sources, localized melting, and microstructural evolution upon solidification. Applying metal powder–based AM in producing structurally sound, defect-free, and reliable parts requires an in-depth understanding of existing printing techniques, the physical and chemical processes involved during printing, feedstock materials, process control methods, and underlying mechanisms of common defects and their prevention.

Metal powder–based AM excels in the following aspects: (i) its ability to recycle feedstock materials, (ii) its relatively high manufacturing accuracy as compared to wire- and sheet-printing, and (iii) the capacity of certain powder–based AM processes (MBJ and EBM) to print parts without requiring support structures because of the support provided by the surrounding unfused or partially melted powder particles. Notably, metal powder–based AM plays an indispensable role in various domains, including the aerospace, biomedical, automotive, molding and tooling, energy, jewelry, marine, oil and gas, and repair and remanufacturing industries.

1.4 Post-Processing

It is challenging to employ metal powder–based AM to directly fabricate parts with properties and surface characteristics that satisfy application requirements. Most metal powder–based AM techniques require post-processing treatment to obtain the desired properties in the printed parts (ISO and ASTM International 2015). Post-processing is crucial for addressing the main issues of AM parts, such as high surface roughness, high porosity, dimensional deviations with respect to the models, and substandard mechanical properties for industrial applications.

In certain metal powder–based AM processes (PBF and DED), a metal substrate where parts can be printed onto is often required. Therefore, the post-processing process of wire cutting, typically using electric discharge machining (EDM) which generates a pulse discharge between a tool electrode and a target object (comprising printed parts and the substrate) for cutting, is required to separate the printed parts from the substrate. This process is also commonly employed to assign desired geometries to printed parts for various purposes (e.g. tensile, fatigue, or fracture toughness testing).

Table 1.2 Post-processing for metal powder–based AM.

Categories	Representative techniques
Surface quality improvement	Manual grinding
	Machining
	Sandblasting
	Shot peening
	Mechanical polishing
	Chemical polishing
	Chemical etching
	Laser shock peening
	Laser polishing
Residual stress relief and defect reduction	Stress relief annealing
	Hot isostatic pressing
Aesthetic improvement	Spray painting
	Electroplating

Table 1.2 exhibits representative post-processing techniques for metal powder–based AM. In accordance with their respective objectives, these techniques can be classified into the categories of surface quality improvement, residual stress relief and defect reduction, and aesthetic improvement.

1.4.1 Surface Quality Improvement

Printed metal components typically undergo post-processing treatment to improve their surface quality (i.e. reduction in surface roughness), which includes manual grinding, machining, sandblasting, shot peening, mechanical and chemical polishing, chemical etching, laser shock peening, and laser polishing.

Manual grinding typically involves abrasive sandpapers with different grit sizes. However, such treatment is only applicable for prototypes or small batches of parts due to its low repeatability and high dependence on the skill of the operator. In addition, any support structures attached to the parts (e.g. overhangs) should first be removed before the grinding process.

Machining utilizes power-driven machines and cutting tools to reduce the surface roughness of printed parts. In particular, CNC is a commonly adopted precision machining process characterized by stable machining quality and high flexibility, machining accuracy, and productivity. Notably, CNC allows for the customization of control programs in each working task to establish control over various tools (e.g. lathes, milling machines, and grinders) in reducing the surface roughness of printed parts.

Sandblasting is the process of removing rust, oxides, and oil contaminants from a surface with high-speed sand (e.g. copper ore sand, emery sand, quartz sand, or iron sand) propelled by compressed air. Sandblasting operations can be categorized

into dry-type sandblasting and liquid blasting processes. The dry-type sandblasting involves pure abrasive propellants capable of removing large amounts of surface material without contamination. In contrast, liquid blasting utilizes a mixture of abrasives and liquid, which removes only small amounts of material but introduces contamination to the parts.

Shot peening is a cold working process that bombards the surface of a material with a stream of small shots (i.e. spherical particles of metal or ceramic) with controlled intensity and coverage. It can increase surface hardness and extend the service life of a part by creating an induced compressive stress layer to enhance its fatigue resistance. Additionally, the surface roughness of printed parts can be reduced and their surface grains can be refined. The shot peening process is commonly performed using air blast systems or centrifugal blast wheels.

Polishing is the process of creating a smooth and specular surface through mechanical or chemical methods. Mechanical polishing methods include magnetically driven abrasive polishing, hydrodynamic cavitation abrasive finishing, and ultrasonic cavitation abrasive finishing.

Magnetically driven abrasive polishing utilizes a slurry comprising magnetic and abrasive materials in a viscous liquid to polish a surface. Hydrodynamic cavitation abrasive finishing is a novel surface modification process employing hydrodynamic cavitation along with abrasives to remove surface irregularities and decrease the surface roughness of a workpiece. In ultrasonic cavitation abrasive finishing, the application of ultrasound and micro-abrasives produces a synergistic effect, in which the former induces the cavitation effect to remove partially melted powder particles on a surface, while the latter serves as bubble nucleation sites to increase the overall cavitation intensity, which further contributes to gradual surface erosion through high-velocity abrasive collisions.

In chemical polishing, a ground sample is immersed in a polishing agent or swabbed with a chemical solution until a clean surface is obtained. Electropolishing is a representative electrochemical polishing process for producing smooth surfaces, and it is accomplished by creating an electrochemical cell in which the printed part is charged anodically. A varying current density is established across the material surface, and it is higher at the peaks and lower at the valleys of the surface topography. The relatively high current density at the protruding points on the surface causes these sites to rapidly dissolve, which levels the surface. However, the effectiveness of electropolishing is limited by the accessibility of counter electrodes in printed parts containing tight spaces and exhibiting complex geometries.

Chemical etching is a post-processing treatment in which chemical reactions occur at the interface between a printed part and a chemical solution, leading to changes in the former's surface roughness. This approach is particularly applicable for treating printed parts with open porous structures.

Laser-based treatment methods utilize laser sources to remove materials and improve the surface accuracy of AM metal parts. Laser-based treatment includes laser shock peening and laser polishing.

In laser shock peening, a pulsating laser beam is directed onto the surface of a metal part, generating shock waves induced by the ablation of a sacrificial layer on the surface. These shock waves travel throughout the surface layer of the part

to cause surface grain refinement and plastic deformation and induce compressive residual stress, which improves the resistance of a material toward fatigue crack initiation and propagation. The underlying mechanism of residual stress generation is similar to that of conventional shot peening, and plastic compression is achieved by the passage of shock waves.

Laser polishing, also known as laser remelting, can enhance the surface accuracy of AM parts while avoiding ablation. In this process, a high-power laser source irradiates the material surface with low-frequency pulses at high scanning speeds to induce local surface melting on the order of nanometers to micrometers. Laser remelting is an eco-friendly process that can improve surface accuracy and reduce surface porosity without incurring any loss of surface materials.

1.4.2 Residual Stress Relief and Defect Reduction

Parts printed by metal powder–based AM processes such as PBF and DED are often subjected to residual stress, which must be relieved through heat treatment before the parts are suitable for industrial usage. The most commonly adopted heat treatment is stress relief annealing, which is a special annealing process that minimizes the residual stress within printed metal parts. This treatment is conducted by heating the parts to a specific temperature below their recrystallization temperature followed by air-cooling. Low-temperature stress relief annealing has a low impact on the microstructure and mechanical properties of a material (Wang et al. 2016), while high-temperature stress relief annealing may refine grains, produce a low dislocation density, and alter the mechanical properties of a material (Xiong et al. 2017). Therefore, low-temperature stress relief annealing is preferable to high-temperature stress relief annealing because it is desirable not to change the microstructure of printed parts during the annealing process.

Hot isostatic pressing (HIP) heat treatment, a thermomechanical treatment process involving the simultaneous implementation of a high temperature (up to 2000 °C) and high isostatic pressure (up to 200 MPa) in a specially constructed vessel with gas as the pressure-transmitting medium, is employed to reduce the porosity of printed parts and improve their densification. Argon gas is the most common pressure-transmitting medium in HIP. Under a high temperature and pressure, the internal pores within a printed part tend to collapse, thereby leading to its densification.

The principal factor distinguishing HIP from other heat treatment techniques is its use of an inert gas as a pressure-transmitting medium to produce uniform microstructural changes on the part surface. The isostatic pressure in HIP arises from the gas atoms colliding with the surface of the part, during which each gas atom is akin to the hammer in a forge. These atomic "hammers" reliably and consistently reach the entire part surface, which corresponds to a uniform pressure.

1.4.3 Aesthetic Improvement

Aesthetics is an indispensable aspect of printed parts. Therefore, improving the aesthetic quality of printed products can further increase their value. Generally, the

"appearance, anti-corrosion, anti-aging, and anti-slip" properties of parts should be considered. Commonly employed methods for achieving aesthetic improvement include spray painting and electroplating.

Spray painting is a painting technique in which paint particles are atomized and sprayed onto a surface. It includes various methods such as air gun spraying, electrostatic spray painting, airless gun spraying, automated linear spraying, and automated flatline spraying. Spray painting is often utilized to improve the appearance of a printed part by applying a smooth and flat coating of the desired color(s) on its surface.

Electroplating is a process that applies a metal coating on a part by external electric fields. In a salt solution containing the metal, the cations of the metal are reduced to atoms through the electrode reaction, and the atoms are subsequently deposited on the surface of the part (that acts as the cathode) to form the coating. Aside from enhancing the appearance of printed parts, the electroplating process can improve their resistance to oxidation, wear, and corrosion, as well as their electrical conductivity. Metals such as chromium, zinc, copper, and nickel are applicable for electroplating.

1.5 Powder Properties and Characterization Methods

Powders form the basis of powder–based AM, and their quality determines the printability and performance of the final parts. While the Technical Committee 119 of ISO has developed and published numerous standards for powder metallurgy since 1967, no standard defined specifically for powder–based AM exists, and thus previously defined metallurgy standards on powder characterization methods are adopted.

Powder sampling must be conducted before any powder characterization can be performed. Sampling methods include scoop sampling, conical pouring and quartering, and chute splitting. In scoop sampling, a scoop of powder is obtained for sampling. Conical pouring and quartering involve pouring the powder onto a flat horizontal surface and dividing the heap into four samples by a cross-shaped cutter. In chute splitting, a chute splitter is employed for sample division. After sampling, a powder can be characterized in terms of its particle morphology, particle size, particle size distribution, density, flowability, chemical composition, and microstructure.

1.5.1 Particle Morphology

The morphology of powder particles can be determined via a standard glossary developed by the British Standards Institute (British Standards 2955 Glossary of Terms Relating to Powders). Particle morphology, which includes shapes and surface features, is dependent on the preparation processes during powder production. The shape of a particle can be described using the following terms: spherical (globular-shaped), acicular (needle-shaped), angular (sharp-edged or roughly polyhedral-shaped), crystalline (a geometric shape freely developed in liquid), dendritic (branched crystalline-shaped), fibrous (regularly or irregularly thread-like),

Table 1.3 Summary of particle size indices and particle shape indices and their descriptions.

Particle size index	Description
Martin's diameter	Length of the line that bisects the area of the particle image (all particles are measured in the same direction).
Feret's diameter	Maximum length of a particle measured in a fixed orientation.
Projected area diameter	Diameter of a circle with the same area as the 2D image of a particle.
Longest diameter	Maximum diameter of a particle.
Perimeter diameter	Diameter of a circle having the same circumference as the perimeter of a particle.
Maximum horizontal intercept	Length of the longest line that can be drawn through a particle in a fixed direction.
Particle shape index	**Description**
Elongation factor	Aspect ratio that is the ratio of the side lengths of an enveloping rectangle that has the minimum area around the cross-section of a particle.
Bulkiness factor	Ratio of the area of a projected particle to the area of the enveloping rectangle.
Surface factor	Sphericity that is used to compare the surface of a particle and the surface of a sphere of equivalent volume.

lamellar (plate-like), granular (equidimensional but irregularly shaped), irregular (lacking symmetry), or modular (round but irregularly shaped).

Table 1.3 summarizes the particle size indices and particle shape indices that can be used to quantitatively describe the morphology of a particle (Allen 1997). Figure 1.2 presents representative surface features and defects of powder particles, which include "splat caps", pores, elongated shapes, breakage, agglomeration, irregular shapes, and small satellites (Mostafaei et al. 2021).

The morphology of powder particles can be characterized by optical microscopy and scanning electron microscopy (SEM). Optical microscopy allows for the counting and measurement of particles at maximum magnification values ranging from 500 to 1500, depending on the model of the apparatus used. Meanwhile, a typical SEM is applicable for imaging surface features with a magnification of up to 3×10^6 and at a resolution of tens of nanometers, thereby enabling the evaluation of grain sizes and second phases on unetched surfaces. Furthermore, when equipped with a backscatter electron detector, an SEM device can facilitate the observation of microstructures on unetched surfaces.

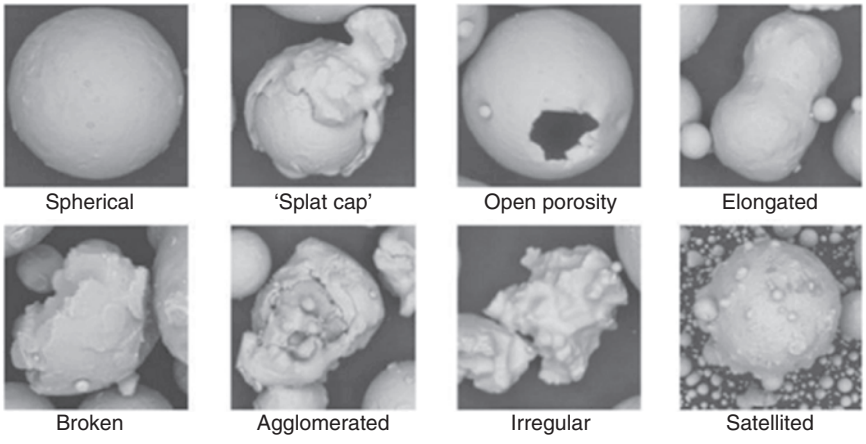

Figure 1.2 Micrographs of powder particles exhibiting various surface features and defects. Source: Mostafaei et al. (2021)/reproduced with permission from Elsevier.

1.5.2 Particle Size Distribution

The particle size distribution of an AM powder is one of its most important characteristics. A volume distribution with respect to particle size can be plotted, as shown in Figure 1.3. The area under the distribution curve to the left of the vertical line $x = D_i$ corresponds to the percentage of the total powder particles that are of sizes smaller than or equal to a specific size gauge D_i. For example, $D_i = 20\,\mu m$ indicates that $i\%$ of all particles are smaller than or equal to 20 μm. The size gauges D_{10}, D_{50}, and D_{90} are the most commonly used indicators. The span, given by $(D_{90} - D_{10})/D_{50}$, is sometimes selected to represent the width of a Gaussian particle size distribution. Additionally, the mean, median, and mode of a particle size distribution, which

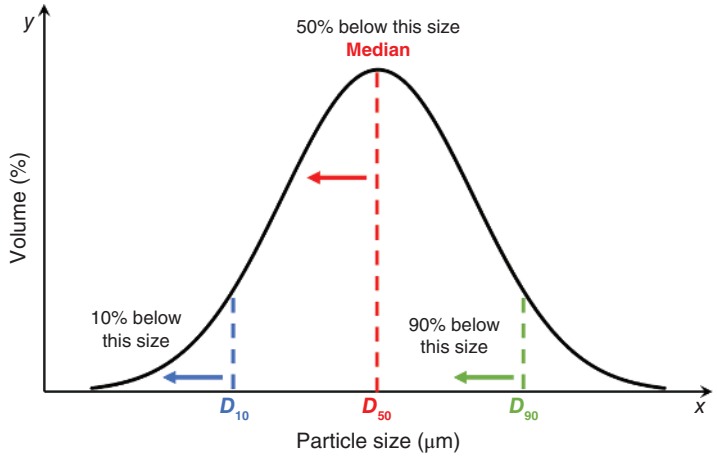

Figure 1.3 Particle size distribution curve showing the size gauges D_{10}, D_{50}, and D_{90}.

correspond to the average particle size, D_{50}, and the peak of the distribution curve, respectively, can be determined.

Particle size distribution is typically measured by the laser diffraction method. This method serves as a convenient and rapid analysis for a broad range of particle sizes. A typical laser diffraction measuring instrument contains a laser source, a particle dispersion module, a particle delivery module, and a detector. When the laser beam is blocked by a particle, part of the light scatters. An angle between the propagation direction of the original and scattered light is formed. A larger particle size results in a smaller angle. Upon being illuminated by parallel laser beams, particles of the same size in a sample deflect light at an identical angle. The scattered light is directed onto a sensor located on its focal plane, forming a series of concentric rings. The intensity of each ring, which corresponds to a specific angle of scattering, is measured to evaluate the volume size distribution of the constituent particles of the sample.

The particle size distribution of a sample can also be quantitatively measured from images captured by optical microscopy or SEM. The images of the constituent particles are usually post-processed before their equivalent diameters are determined, and the entire procedure may be time-consuming. An SEM machine developed by ASPEX Corporation is equipped with an automated feature analysis module, which is capable of quantifying the sizes of thousands of particles within several hours.

Sieve analysis, which involves the separation of particles according to their sizes, is also commonly employed to obtain the particle size distribution of a sample owing to its simplicity and low cost. A typical sieving unit comprises a series of sieves stacked on top of a shaker exhibiting rotary and tapping motions, with each sieve incorporating a phosphor bronze or stainless steel wire mesh cloth woven in a square mesh pattern. The sieves are stacked in the order of decreasing mesh sizes, with the sieve possessing the largest mesh size on top. Standard sieve sizes are specified in ISO standards 565 and 3310/1, ASTM standard E 11, and CIS standard GOST 3584.

1.5.3 Density

The packing density of a powder bed is defined as the ratio of the volume of its constituent powder particles to its total volume. It is a key parameter for assessing the packing efficiency of a powder bed in AM. A powder bed with a large packing density minimizes the porosity of the printed parts, thereby improving their mechanical properties. The packing density of a powder bed is influenced by a variety of factors such as the characteristics of the powder particles (size, size distribution, and shape), bulk properties (e.g. Young's modulus and hardness), and powder spreading parameters (powder layer thickness and spreading velocity). For bimodal powder mixtures containing both small and large particles, the maximum packing density can be achieved with specific ratios of the two types of powder particles, as shown in Figure 1.4.

The apparent density of a powder, with units of g/cm^3, is defined as the mass per unit volume of its loose powder particles. The Hall funnel method is the most prevalent method for measuring the apparent density of a powder, and the powder is

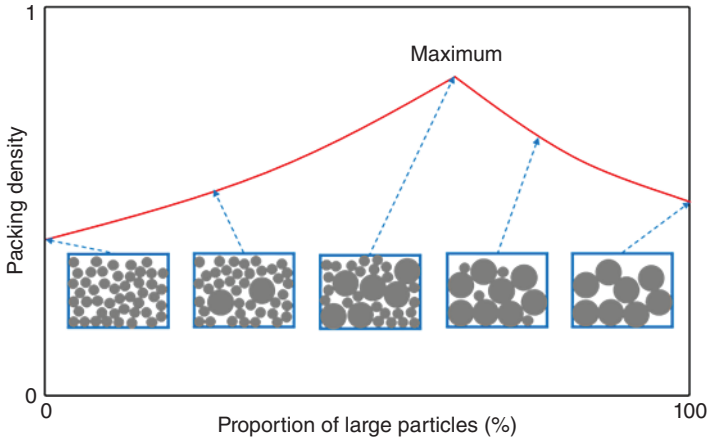

Figure 1.4 Variation of the packing density with the proportion of large powder particles for bimodal powder mixtures. Source: Adapted from German (1992).

poured through a funnel to fill a 25 cm^3 container. The apparent density is obtained by dividing the mass of the contents in the container by its volume. Generally, the apparent density of a powder decreases with its particle size and increases with its particle surface roughness. A powder with a wide size distribution possesses a relatively high apparent density since the space between its coarse powder particles is filled by smaller powder particles.

The tap density of a powder is defined as its density when its container is tapped or vibrated under specified conditions. The tap density (unit: g/cm^3) of a powder is obtained by dividing the mass of the tapped powder in a container by its volume. ISO 3953 established a method for measuring the tap density of a powder, in which a 100 ml (with increments of 0.2 ml) glass graduated cylinder is typically utilized. The tap density of a powder is dependent on the size distribution, shape, and surface roughness of its particles and is always higher than the free-flow apparent density.

The skeletal density, which is often measured through pycnometric methods, is the true density of a powder in its solid state. In pycnometry, the ratio of the mass of a powder to its volume is determined based on the volumetric displacement of a fluid medium. Gas pycnometry, in which helium or nitrogen is employed as the fluid medium, is commonly practiced since the tiny gas atoms can occupy the defects within a solid powder. Meanwhile, liquid pycnometry provides an alternative approach in which highly penetrative liquids (ethanol, oils, butanol, acetone, etc.) are selected as the fluid medium. The number of defective powder particles exhibiting cracks, satellite particles, and pores can be estimated based on the measured skeletal density of a powder.

1.5.4 Flowability

The flowability of a powder is often construed as its ability to flow in a desired manner. In powder–based AM systems, flowability determines the feeding and spreading

behaviors of a powder. It is influenced by the particle size distribution, density, particle morphology, and moisture content of the powder. For example, fine powder particles (smaller than 10 μm) typically flow poorly and may even become stuck, while a powder that contains both fine and large particles exhibits good flowability. Due to its relative ease of measurement and correlation to powder flow behaviors, the Hausner ratio of an AM powder, expressed as its tap density divided by its apparent density (Hausner 1967), is commonly used to quantify its flowability. Since both the apparent and tap densities are related to interparticle friction, the Hausner ratio also represents interparticle friction, which directly influences flowability. Generally, a Hausner ratio smaller than 1.25 corresponds to a free-flowing powder.

The flowability of a powder can be assessed based on its flow time, which is defined as the duration for 50 g of the powder to flow through a funnel with a 2.5 mm diameter opening under the influence of gravity (Hall flowmeter). The flow time of a powder is expressed in units of g/s and can be readily compared with those of different powders for a quick assessment of its flowability. Another common flowability parameter is the angle of repose α, which is defined as the angle between a horizontal surface and the slope of a powder heap (Figure 1.5). To measure this parameter, a powder is allowed to fall freely, typically through a fixed funnel, and deposited onto a horizontal surface. Similarly to the Hausner ratio, the angle of repose is related to interparticle friction and cohesion, and a large angle of repose indicates poor powder flowability.

Spherical powder particles usually exhibit better flowability than their irregularly shaped counterparts. A high moisture content can increase powder stickiness and reduce powder flowability. Therefore, it is recommended to dry the powder before printing. Although the flowability of a powder is mostly an intrinsic property, it is also dependent on the interactions between the powder and the environment of AM systems. The interactions between a powder and various AM systems thus contribute to different powder flow behaviors. Therefore, extensive testing with respect to different AM equipment is necessary to evaluate powder flowability.

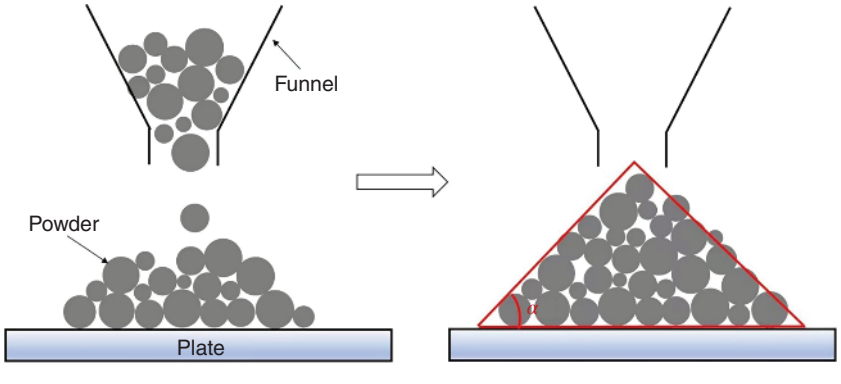

Figure 1.5 Schematic of a fixed funnel method for measuring the angle of repose of a powder.

1.5.5 Chemical Composition

The chemical composition analysis of a powder involves both surface and bulk analyses. Surface analysis methods include energy dispersive spectroscopy (EDS), electron probe microanalysis (EPMA), auger emission spectrometry (AES), X-ray photoelectron spectrometry (XPS), and secondary ion mass spectrometry (SIMS). Meanwhile, bulk analysis methods cover atomic absorption spectrometry (AAS), inductively coupled plasma atomic emission spectroscopy (ICP–AES), X-ray fluorescence (XRF), infrared (IR) spectroscopy, and inert gas fusion. These two categories of analytical methods are further elaborated in the following subsections.

1.5.5.1 Surface Analysis Methods

When coupled with SEM, EDS can be utilized to identify chemical compositions on the microscale and evaluate the chemical composition on a particle surface. Since a SEM/EDS system requires conductive samples, this method is more suitable for evaluating the particle size and chemical composition of metal powders than polymer powders. Meanwhile, EPMA provides qualitative and quantitative analyses for elements with atomic numbers greater than or equal to 11 (Na) with detection limits of approximately 1 μm. However, the detection sensitivity of EPMA is relatively poor for light elements with atomic numbers ranging from 5 (B) to 10 (Ne).

AES can facilitate the compositional analysis of almost every element (except H and He) on a powder surface with a sensitivity of 0.1–1.0 at.%. Meanwhile, XPS, a surface-sensitive quantitative spectroscopic method based on the photoelectric effect, can be conducted in tandem with ion-etching to identify the elements constituting the surface of a material and their chemical states, as well as the overall electronic structure and density of electronic states within the material. Finally, a variety of information pertaining to the surface, subsurface, or bulk composition of a powder can be acquired through SIMS, with a detection limit in the parts per billion (ppb, in units of ng/ml^3) to parts per million (ppm, in units of μg/ml) range for elements.

1.5.5.2 Bulk Analysis Methods

The AAS method is one of the most commonly employed methods for trace element analysis. It is capable of detecting the element content in a powder with a detection limit in the ppb range. This method is established based on the transition of higher orbital electrons of a gaseous atom from the ground state to an excited state upon absorbing radiation of a specific wavelength. Thus, it can qualitatively and quantitatively analyze an element based on its absorption spectra with respect to a ground-state atomic vapor.

ICP–AES can detect over 70 elements (not Ar), with detection limits ranging from the ppm to ppb range, with most samples being aqueous solutions at higher levels of accuracy. This method utilizes plasma as an excitation light source, and multiple elements can be detected simultaneously. In an ICP–AES system, the sample is first atomized and subsequently enters a plasma channel in the form of an aerosol. Finally, the aerosol sample is fully vaporized, ionized, and excited in

a high-temperature inert atmosphere, thereby emitting radiation corresponding to the characteristic spectra of its constituent elements, from which the element content can be determined.

XRF is an efficient and nondestructive method that employs high-energy X-rays or gamma-rays to bombard a sample and induce the emission of secondary X-rays characterized by its constituent elements. These secondary X-rays are captured by a detector installed within an XRF system, which converts such signals into useful information regarding the element content of the sample. This method has a resolution limit of approximately 100 ppm.

IR spectroscopy is usually performed to identify functional groups in organic molecules, and the samples can be in the form of solids, liquids, or thin films. In the sample, molecular vibrations, in the form of stretching and bending of covalent bonds, occur at specific frequency values, which correspond to troughs in the IR spectra. Specific chemical bonds and functional groups in the sample are identified based on these troughs. IR spectroscopy has also been employed to characterize surface oxides on metal specimens (Jasinski and Iob 1988). Oxidation of a powder, particularly metal powder, is detrimental to powder–based AM processes. When a metal powder melts during the printing process, oxide layers form on the powder surfaces due to oxidation and hinder the consolidation of the printed parts, thereby resulting in the so-called "balling effect". Hardened oxide films also impede proper surface wetting and lead to poor adherence of the printed layers, which may induce porosity in the printed parts. Another type of powder contamination exists in the form of hydroxide films, which typically form on powder surfaces due to their ability to absorb moisture under high humidity. In contrast to solidified oxide layers that are often hard and brittle, hydroxide films are generally highly viscous. Therefore, the hydroxide films increase the tendency of particles to agglomerate and inhibit particle flow within the powder bed. Finally, irradiation of water layers adsorbed onto powder surfaces facilitates the dissociation of hydrogen atoms from the water molecules, and entrapped gas pores are formed upon the solidification of the melt pool, causing melt pool sputtering.

Inert gas fusion is a quantitative method for measuring the contents of H, N, and O elements in metal samples (Holt and Goodspeed 1963). Samples are first weighed and placed in a graphite crucible, in which they are heated to a molten state. Meanwhile, H_2, N_2, and O_2 molecules released from the samples are separated to evaluate the weight percentage of each element.

1.5.6 Microstructure

X-ray diffraction (XRD) is an X-ray spectrographic method primarily for identifying crystal structures and properties, including the number of phases in a metal powder sample, with a sensitivity of 3–5 vol.% for each phase component. During XRD analysis, a sample is bombarded with X-rays at different incident angles θ, and the intensity of the diffracted X-rays is measured. Constructive interference of the diffracted X-rays results in the formation of distinguishable intensity peaks. The condition for constructive interference to occur is described by Bragg's law, $n\lambda = 2d\sin\theta$,

where n is the diffraction order (an integer), λ is the wavelength of the incident radiation, and d is the spacing between successive crystal planes (Skoog et al. 2006). By incorporating the knowledge of reflection angles for specific phases and indexing the positions of the peaks, the crystal structure of a sample can be determined.

Focused ion beam (FIB) microscopy is a technique for imaging and milling material surfaces, in which a beam of cations is utilized to form a raster image of a surface or to remove layers from it. Typically, a dual FIB/SEM approach is adopted for powder characterization, in which the FIB setup is mainly employed for milling purposes. Such an approach can also be undertaken to directly visualize the internal grain structure and porosity of powder particles.

Transmission electron microscopy (TEM) is a highly effective analytical tool for imaging a phase in powder form to obtain specific information (size and shape of the phase particles, crystallographic orientation, etc.). In TEM analysis, the specimens must be processed to reach a size of less than 100 nm to be electron transparent. Various specimen preparation methods are available, which include bulk preparation by thinning and dimpling and final polishing by an ion polisher or via electropolishing. A more advanced method for preparing TEM samples is to conduct FIB microscopy in conjunction with SEM to retrieve a sample from a bulk specimen, which is subsequently attached to a copper or molybdenum grid that can be inserted into the TEM facility. The obtained TEM diffraction patterns can be used to determine whether a material is a single crystal (sharp diffraction patterns), polycrystalline (diffraction rings), or amorphous (hazy rings).

Electron backscatter diffraction (EBSD) is a scanning electron microscope-based microstructural-crystallographic characterization method commonly employed when studying crystalline or polycrystalline materials. This method can provide details on the structure, crystal orientation, phase, and strain in powder materials. During an EBSD measurement, a flat and polished crystalline specimen is placed at a largely tilted angle (about 70° relative to the normal incidence of the electron beam) in an SEM chamber. A camera, equipped with a phosphor screen and integrated with a digital frame grabber, is inserted into the chamber and approaches the surface of the inclined specimen. The sample is then bombarded by electrons, which may backscatter and exit at various Bragg's angles, thereby undergoing diffraction and forming Kikuchi bands corresponding to different diffracting crystal planes of the lattice. As a result, the microstructural maps of the sample, which spatially describe its crystal orientation, can be obtained and utilized to examine the micro-texture of the sample. Such maps provide abundant information about a sample, such as its grain orientation, grain boundary, and grain size distribution. Additionally, various statistical tools can also be used to evaluate the average misorientation, grain size, and crystallographic texture of the sample.

Thermal analysis methods are mainly employed for tracking changes in the chemical properties of a sample over a range of temperatures, and they include thermogravimetric analysis (TGA), differential thermal analysis (DTA), and differential scanning calorimetry (DSC). These methods also reveal information regarding the exothermic and endothermic events that occur within the sample. In TGA, the mass of a sample is recorded as a function of temperature, which provides information

on its content according to the loss of volatile elements and the potential formation of oxides. In addition, TGA allows for *ex situ* analysis of the response of a powder subjected to increasing temperatures during PBF processes. Meanwhile, DTA is a qualitative method in which a sample and an inert reference material are simultaneously heated, and the temperature difference between them is recorded as a function of temperature or time, which can be used to identify potential phase transitions. Generally, DTA analysis is also complemented by TGA and DSC. Finally, DSC is a quantitative method that records the difference in heat capacity between the sample and a reference material as a function of temperature.

1.6 Challenges and Future Trends of Metal Powder–Based AM

Present challenges and future trends of metal powder–based AM are centered on developing printing materials and processes, *in situ* monitoring, numerical simulations, and standardization.

The main challenges surrounding the development of printing materials are present in the following aspects: (i) tuning the powder composition to achieve the desired properties of the final parts (e.g. multifunctional, strong, ductile, and lightweight); (ii) controlling the stresses and distortion within the printed parts; (iii) achieving a comprehensive understanding of metallurgical principles; (iv) tuning microstructures and properties in different regions of a printed part by manipulating process parameters and ensuring reproducibility; (v) reducing anisotropy in the mechanical properties of the printed parts; (vi) preventing the formation of metallurgical defects; and (vii) establishing a database of printable materials. In addition, the lack of specialized metal powder preparation processes hinders the standardization of AM powder properties (see Chapter 2 for further details).

Large-scale manufacturing, hybrid manufacturing, and multiple-energy-source-aided manufacturing are projected to be popular future research trends concerning the development of printing processes. For example, large-scale PBF manufacturing utilizes multiple laser sources and optical systems to fabricate parts extensively. Hybrid manufacturing refers to the integration of a powder–based AM technique (PBF or DED) with a subtractive manufacturing system (e.g. milling or grinding), offering a significant improvement of the printed parts in terms of their dimensional accuracy and surface quality. Multiple-energy-source-aided manufacturing incorporates external energy fields (e.g. electromagnetic fields, ultrasonic fields, and electric fields) into a powder–based AM system. Such energy fields induce strong vibrations within the melt pools during the printing process, which can effectively refine the microstructures of the printed parts and reduce metallurgical defects within them.

The challenges of quality control during printing processes primarily lie in the areas of *in situ* monitoring, process sensing, and adaptive control, which are critical in regulating such processes to achieve high productivity while avoiding common defects in the printed parts. For example, a key aspect of process control is the availability of well-tested real-time models that serve as media for relating the process

variables with the desired properties. Notably, adequately standardized phenomenological modeling can reveal the most important factors that affect the quality of metal parts, such as temperature and velocity fields, cooling rates, and solidification parameters. Therefore, it is a powerful tool for assessing the effects of process variables on part quality prior to production. Furthermore, the development and testing of phenomenological models provide a solid foundation for the eventual construction of digital twins of physical objects in metal powder–based AM. With the incorporation of genetic algorithms and other global search algorithms, the utility of such digital twins can be greatly expanded to tailor part attributes, optimize production variables, reduce defects, and improve part quality. However, refining such virtual representations requires considerable time, effort, and resources.

Contemporary numerical simulations of AM are primarily conducted to provide insights on powder-spreading behaviors on the powder bed and heat transfer phenomena, residual stress development, distortion, microstructure evolution, and porosity formation in AM parts. However, there appears to be a lack of agreement regarding the characteristics of an acceptable model since the efficacy of each model is assessed according to its computational cost and/or the accuracy of its corresponding results. Such criteria are difficult to implement due to the different resources available in each research project and the variations between model outputs.

AM modeling research is directed at understanding the underlying mechanisms governing different phenomena, developing a computational model for describing specific processes, and establishing a process–structure–property relationship. One should note that adopting a feedback-based approach is necessary, in which earlier simulation results are utilized in subsequent simulations until a model has successfully satisfied specific requirements (low distortion, desired microstructure, high cycle fatigue, etc.).

Material–structure–performance integrated AM could be explored to achieve high-performance and multifunctional AM parts (Gu et al. 2021). Such technology relies on developing more digitized materials and structures, which could be accomplished with the Materials Genome Initiative, standardization of formats, and a systematic printability database. High mechanical performance and multifunctionality can be simultaneously achieved for an AM metal part through the innovative design of materials and structures.

The standardization of metal powder–based AM is impeded by critical challenges spanning many aspects, which include cost, design, software, materials, traceability, machine constraints, printing process monitoring, mechanical properties, repeatability, scalability, validation, standards, quality, inspection, post-processing, and tolerances. A primary challenge is the unsatisfactory development of qualification and certification process for various AM applications because of high costs, long lead times, and inadequate standards, rules, and regulations. Other challenges arise due to the lack of *in situ* measurements for real-time closed-loop process control systems, insufficient data, and poor process reliability and repeatability due to limited research on heat source–powder interactions, heat transfer, vaporization, defect formation, quantitative metallography, etc. Moreover, the large-scale production of AM parts using commercially available AM equipment is highly difficult.

While the market expansion of AM technologies requires increased standardization and improved quality control of AM products, a more comprehensive understanding of the printing processes and practical innovations must first be achieved.

Despite being a revolutionary method for facilitating customized part fabrication and niche applications, metal powder–based AM requires further research and development to achieve the mass production of parts at a reduced cost.

1.7 Summary

This chapter briefly discusses the development of AM technology, popular metal powder–based AM techniques, post-processing methods, representative metal powder characteristics and their characterization methods, and challenges and future trends of metal powder–based AM.

AM technology is classified into seven broad categories, i.e. vat photopolymerization, material jetting, material extrusion, PBF, DED, binder jetting, and sheet lamination techniques. Among them, PBF, DED, and binder jetting are the predominant powder–based AM techniques. In particular, LPBF, EBM, L-DED, and MBJ are the most commonly adopted powder–based AM processes for printing metal parts.

Most metal powder–based AM products require post-processing to obtain the desired properties. Surface quality improvement methods include manual grinding, machining, sandblasting, shot peening, mechanical and chemical polishing, chemical etching, laser shock peening, and laser polishing. In addition, heat treatment methods, such as stress relief annealing and HIP, can be employed to minimize residual stress within the printed parts and reduce their porosity. Finally, aesthetic improvement approaches include spray painting and electroplating.

Powders are the principal component of powder–based AM, and they are characterized in terms of their morphology, size, size distribution, density, flowability, chemical composition, and microstructure. The quality of a powder is determined by these characteristics, which determine the printability and performance of the final parts.

Present challenges and future trends of metal powder–based AM are proposed in terms of developing printing materials and processes, *in situ* monitoring, numerical simulations, and standardization. Furthermore, as a revolutionary method for facilitating customized part fabrication and certain niche applications, metal powder–based AM technologies require further development to mass-produce parts at a reduced cost.

References

Allen, T. (ed.) (1997). *Particle Size Measurements*, 5e. Berlin: Springer.

Bermingham, M.J., Kent, D., Zhan, H. et al. (2015). Controlling the microstructure and properties of wire arc additive manufactured Ti–6Al–4V with trace boron additions. *Acta Materialia* 91: 289–303.

Chua, C.K. and Leong, K.F. (2017). *3D Printing and Additive Manufacturing: Principles and Applications*, 5e. Singapore: World Scientific.

Dehoff, R.R. and Babu, S.S. (2010). Characterization of interfacial microstructures in 3003 aluminum alloy blocks fabricated by ultrasonic additive manufacturing. *Acta Materialia* 58 (13): 4305–4315.

Gebler, M., Uiterkamp, A.J.S., and Visser, C. (2014). A global sustainability perspective on 3D printing technologies. *Energy Policy* 74: 158–167.

German, R.M. (1992). Prediction of sintered density for bimodal powder mixtures. *Metallurgical Transactions A* 23 (5): 1455–1465.

Gibson, I., Rosen, D., and Stucker, B. (2014). *Additive Manufacturing Technologies: 3D Printing, Rapid Prototyping, and Direct Digital Manufacturing*, 2e. Berlin: Springer.

Gu, D., Shi, X., Poprawe, R. et al. (2021). Material-structure-performance integrated laser-metal additive manufacturing. *Science* 372 (6545): eabg1487.

Han, C., Babicheva, R., Chua, J.D.Q. et al. (2020a). Microstructure and mechanical properties of (TiB+TiC)/Ti composites fabricated in situ via selective laser melting of Ti and B_4C powders. *Additive Manufacturing* 36: 101466.

Han, C., Fang, Q., Shi, Y. et al. (2020b). Recent advances on high-entropy alloys for 3D printing. *Advanced Materials* 32 (26): 1903855.

Hausner, H.H. (1967). Friction conditions in a mass of metal powder. *International Journal of Powder Metallurgy* 13 (4): 7–13.

Holt, B.D. and Goodspeed, H.T. (1963). Determination of nitrogen, oxygen, and hydrogen in metals by inert gas fusion. A manometric method. *Analytical Chemistry* 35 (10): 1510–1513.

Hull, C.W. (1986). Apparatus for production of three-dimensional objects by stereolithography. US Patent 4,575,330, filed 08 Augst 1984, issued 11 March 1986.

ISO and ASTM International (2015). ISO/ASTM 52900: Additive manufacturing – General principles – Terminology.

Jasinski, R. and Iob, A. (1988). FTIR measurements of iron oxides on low alloy steel. *Journal of the Electrochemical Society* 135 (3): 551.

Kelly, B.E., Bhattacharya, I., Heidari, H. et al. (2019). Volumetric additive manufacturing via tomographic reconstruction. *Science* 363 (6431): 1075–1079.

Kuang, X., Wu, J., Chen, K. et al. (2019). Grayscale digital light processing 3D printing for highly functionally graded materials. *Science Advances* 5 (5): eaav5790.

Li, B., Zheng, H., Han, C., and Zhou, K. (2021). Nanotwins-containing microstructure and superior mechanical strength of a Cu-9Al-5Fe-5Ni alloy additively manufactured by laser metal deposition. *Additive Manufacturing* 39: 101825.

Martin, J.H., Yahata, B.D., Hundley, J.M. et al. (2017). 3D printing of high-strength aluminium alloys. *Nature* 549 (7672): 365–369.

Mostafaei, A., Kimes, K.A., Stevens, E.L. et al. (2017). Microstructural evolution and magnetic properties of binder jet additive manufactured Ni-Mn-Ga magnetic shape memory alloy foam. *Acta Materialia* 131: 482–490.

Mostafaei, A., Elliott, A.M., Barnes, J.E. et al. (2021). Binder jet 3D printing – process parameters, materials, properties, modeling, and challenges. *Progress in Materials Science* 119: 100707.

Ribeiro, I., Matos, F., Jacinto, C. et al. (2020). Framework for life cycle sustainability assessment of additive manufacturing. *Sustainability* 12 (3): 929.

Saha, S.K., Wang, D., Nguyen, V.H. et al. (2019). Scalable submicrometer additive manufacturing. *Science* 366 (6461): 105–109.

Skoog, D.A., Holler, F.J., and Crouch, S.R. (2006). *Principles of Instrumental Analysis*, 6e. Boston: Cengage Learning.

Tan, L.J., Zhu, W., and Zhou, K. (2020). Recent progress on polymer materials for additive manufacturing. *Advanced Functional Materials* 30 (43): 2003062.

Truby, R.L. and Lewis, J.A. (2016). Printing soft matter in three dimensions. *Nature* 540 (7633): 371–378.

Tumbleston, J.R., Shirvanyants, D., Ermoshkin, N. et al. (2015). Continuous liquid interface production of 3D objects. *Science* 347 (6228): 1349–1352.

Walker, D.A., Hedrick, J.L., and Mirkin, C.A. (2019). Rapid, large-volume, thermally controlled 3D printing using a mobile liquid interface. *Science* 366 (6463): 360–364.

Wang, X., Zhang, W., Liu, Z. et al. (2016). Improvement on room-temperature ductility of 6.5 wt% Si steel by stress-relief annealing treatments after warm rolling. *Materials Characterization* 122: 206–214.

Xiong, X., Hu, S., Dang, N., and Hu, K. (2017). Effect of stress-relief annealing on microstructure, texture and hysteresis curve of mechanically cut non-oriented Fe-Si steel. *Materials Characterization* 132: 239–247.

Zhang, D., Qiu, D., Gibson, M.A. et al. (2019). Additive manufacturing of ultrafine-grained high-strength titanium alloys. *Nature* 576 (7785): 91–95.

Zhang, Y., Bai, S., Riede, M. et al. (2020). A comprehensive study on fused filament fabrication of Ti-6Al-4V structures. *Additive Manufacturing* 34: 101256.